Development, Optimization, and Characterization of Electrospun Poly(lactic acid) Nanofibers Containing Multi-Walled Carbon Nanotubes

Seth D. McCullen,[1] Kelly L. Stano,[1] Derrick R. Stevens,[2] Wesley A. Roberts,[2] Nancy A. Monteiro-Riviere,[3] Laura I. Clarke,[2] Russell E. Gorga[1]

[1]*Department of Textile Engineering, Chemistry, and Science, North Carolina State University, Raleigh, North Carolina 27695*
[2]*Department of Physics, North Carolina State University, Raleigh, North Carolina 27695*
[3]*Department of Clinical Sciences, The Center for Chemical Toxicology Research and Pharmacokinetics, North Carolina State University, Raleigh, North Carolina 27695*

Received 22 August 2006; accepted 11 January 2007
DOI 10.1002/app.26288
Published online 25 April 2007 in Wiley InterScience (www.interscience.wiley.com).

ABSTRACT: Electrospinning of poly (L-D-lactic acid) (PLA) was investigated with the addition of multi-walled carbon nanotubes (MWNT) for development of a scaffold for tissue engineering. Through this experiment, it was determined that the optimal concentration of PLA with weight average molecular weight (M_w) 250,000 g/mol is $\sim$ 20 wt % as indicated by scanning electron microscopy. This concentration produces fibers with no beading or film formation. The preferred solvent system is a combination of chloroform and dimethyl formamide to alleviate the volatile action of chloroform. The optimum processing parameters for PLA are an electric field of 1 kV/cm which was determined by a surface response plot to minimize fiber diameter based on the applied voltage, working distance, and addition of MWNT. Fourier Transform infrared spectroscopy has indicated the removal of the solvent system. With the addition of MWNT, the fiber diameter was drastically reduced by 70% to form fibers with a mean diameter of 700 nm. This is believed to be due to an increased surface charge density for the MWNT/polymer solution. Transmission electron microscopy validated the alignment of the MWNT within the fibers. MWNT loading exhibited an increase in the conductance of the scaffold and the tensile modulus at an optimal loading level of 0.25 wt %. J Appl Polym Sci 105: 1668–1678, 2007

Key words: electrospinning; polymers; nanofibers; carbon nanotubes; electrical properties; mechanical properties; electron microscopy

INTRODUCTION

Current research has focused on the fabrication of polymer nanocomposites by incorporating carbon nanotubes into various polymer systems.[1–3] Carbon nanotubes exhibit outstanding physical properties with a large aspect ratio (length/diameter), in the range of thousands, which can reduce the amount of filler needed to obtain significant increases in physical properties (for composite systems it is more advantageous to utilize fillers with an aspect ratio greater than one).[4] Researchers have been able to show that through dispersion and orientation of carbon nanotubes, improved physical properties including Young's Modulus, toughness, tensile strength, and conductivity can be achieved in polymeric matrices.[3,5,6]

Recently, the electrospinning method has been used to provide a means to construct nanocomposites by suspending nanomaterials in polymer solutions and creating fibers with diameters on the nano to micro scale containing the suspended particle.[7–11] The fibers are created by electrostatic repulsion and the coulombic forces because of an external electric field applied to a polymer solution.[12,13] The end result is a randomly oriented mat of reinforced fibers with a high porosity due to the ratio of surface area to volume. This aspect of electrospinning is advantageous for use as a means of production for scaffolds for tissue engineering, by producing a functionalized material with interconnected pores and tremendous surface area that is similar to the scale of the extra-cellular matrix.[14]

Numerous researchers have experimented with the use of electrospun poly(lactic acid) (PLA) as a tissue scaffold by electrospinning because its biocompatibility and degradation properties are well understood.[15–23] It has been noted that drastic morphological changes result as a function of polymer concentration.[17,23] In one study it was not possible to collect continuous fibers at concentrations below 20 wt % or above 40 wt % because of the viscosity of the solution. The researchers hypothesized that fibers produced from 20 to 30 wt % had an apparent

Correspondence to: R. E. Gorga (regorga@ncsu.edu).
Contract grant sponsor: Nanotechnology Initiatives at North Carolina State University.

Journal of Applied Polymer Science, Vol. 105, 1668–1678 (2007)

wetness when deposited on the collector, enabling a solidification of the liquid jet because of the surface tension and relaxation process by the viscoelastic property of the wet fibers.[23] The electrospun nanofibers produced were noncrystalline, but the researchers were able to yield a high orientation by collecting the nanofibers on a rotating drum.[23] Overall the PLA at higher concentrations in solution produced uniform nanofibers at lower electrical fields. Thus, when choosing the specific polymer system it is imperative to understand the role of molecular weight and concentration and how these variables influence the number of entanglements of polymer chains in solution, ultimately dictating the viscosity. This was reported by Tan where the most important processing variables for minimizing fiber diameter were the weight average molecular weight (M_w) and concentration, as well as the electrical conductivity of the solvent system.[18]

Work by Zong et al. demonstrated that drugs could be loaded into nanofibers by suspending them within the polymer solution.[23] With the addition of any particle (anionic, cationic, or nonionic) the fiber diameter and diameter distribution of the electrospun fibers can be significantly reduced.[21] A hypothesis to explain this effect is that particle addition maintains a more uniform charge density within the whipping instability created during electrospinning.

The objective of this research is the development and characterization of electrospun nanocomposites for tissue engineering scaffolds incorporating carbon nanotubes. This work focuses on optimizing the processing parameters for electrospun nanofibers of PLA through response surface methodology (RSM), and the incorporation of a low mass fraction of multi-walled carbon nanotubes (MWNT) into electrospun scaffolds to examine changes in the mechanical and electrical properties.

MATERIALS AND METHODS

Fabrication

The electrospinning apparatus includes a programmable syringe pump obtained from New Era Pump Systems Model NE 500. The high voltage power supply was obtained from glassman high voltage model no. FC60R2 with a positive polarity.

Parameter optimization

The pump operated at a flow rate of 50–200 μL/min. The operating voltage was from 10 to 20 kV with an electric field of 0.5–2 kV/cm. The solutions were loaded into 10-mL syringes with luer-lock connections and used in conjunction with a 4 inch 20-gauge blunt tip needle. The design of the electrospinning set-up was based on a point-plate configuration.

Materials

Poly(L-D-lactic acid) was obtained (Sigma-Aldrich, St. Louis, MO) with a weight average molecular weight (M_w) of 250,000 g/mol and a number average molecular number (M_n) of 100,000 g/mol. Chloroform and dimethyl formamide (Sigma-Aldrich, St. Louis, MO) were used to dissolve the PLA. MWNT were supplied by Nano-Lab and produced by plasma enhanced chemical vapor deposition using acetylene and ammonia with an iron catalyst and grown on a mesoporous silica substrate.[24] The MWNT used had a diameter of 15 ± 5 nm and length of 5–20 μm at 95% purity. The surfactant Pluronic F127 (BASF, Florham Park, NJ) was used to disperse the MWNT.

Methods

PLA was solubilized in chloroform and dimethyl formamide (DMF) at two different ratios of 1: 0 and 3 : 1 respectively. MWNT were sonicated at a concentration of 0.1 mg/mL in DMF with 1% Pluronic F127 (BASF, Florham Park, NJ) using an Ultrasonic Model 2000U generator and needle probe at 25 Hz for 4 h in an ice bath.[25,26] This produced a stock solution for MWNT incorporation into the solubilized PLA. Electrospun nanocomposites containing 0–1 wt % MWNT were produced for physical property analysis.

Characterization

Scanning electron microscopy

For scanning electron microscopy (SEM) a JEOL JSM-6400 FE w/EDS, operating at 5 kV, was used to determine fiber morphology of the electrospun samples. The electrospun samples were coated with Au/Pd ~ 100 Å thick to reduce charging and produce a conductive surface. Digital images were captured at 500×, 5000×, and 10,000× and analyzed using NIH Scion Image™ software for fiber diameter measurements.

Transmission electron microscopy

Transmission electron microscopy (TEM) was performed on a JEOL 100S operating at 80 kV, with samples spun directly on a Cu 400 mesh grid coated with holey thin carbon film. Micrographs were developed, digitally scanned, and were not further modified.

Fourier transform infrared spectroscopy

To determine the presence of the organic solvents a Nicolet Nexus 470 Fourier Transform InfraRed Spectrophotometer (FTIR) was used. Accessories include a single bounce attenuated reflectance device (OMNI Sampler™ with Ge crystal) for identification of contaminants and small particles/fibers. Transmission

and reflectance measurements were performed for qualitative analyses of unknowns. Spectral searches to identify the residual solvents were performed using commercially available libraries from Sigma. Spectroscopy was performed directly after nanocomposite fabrication and 12 h after soaking in phosphate buffered saline (PBS).

Electrical measurements

Current-voltage characteristics of random mats of electrospun fibers with varying MWNT wt % (0–1) were conducted with a Keithley Model 6430 subfemto amp remote source meter. The fibers were electrospun directly onto flat, interdigitated electrodes on glass (fabricated by standard UV-lithography) to form a mat of ~ 1 μm thickness and measured as previously reported.[27] The electrodes had 26-, 1-mm long finger pairs each separated by 10 μm. The use of interdigitated electrodes provides a facile measurement of the extremely porous mat without concern of pin-hole defects in a sandwich-electrode configuration. The low-voltage linear region of the current-voltage characteristic was fit to determine the mat conductance. By examining the conductance versus MWNT loading curve, the critical weight percent associated with the percolation threshold was determined. Before deposition of the mat, blank electrodes had a measured conductance of $\sim 1 \times 10^{-15}$ S, which serves as the lower limit of our measurement range.

Mechanical measurements

Tensile material property tests of electrospun nanocomposites were performed with an Instron Model 5544 using the Bluehill™ Version 1.00 software on samples of 0–1 wt % MWNT at a crosshead speed of 2.00 mm/min. The scaffold thickness was approximated by averaging 10 measurements for each sample and cross-sectional area (A) was calculated as follows:

$$A = t \times w \times v \tag{1}$$

where t is the thickness of the sample, w is the width, and v is the volume percentage of fibers. The volume percentage of fibers or porosity of the scaffolds of each MWNT weight percentage was determined using SEM images and importing into NIH Image J™ Software (Bethesda, Maryland) where they were converted to a four pixel system and the void space calculated. Ten images of each MWNT weight percentage were analyzed.

Statistical analysis

Results are presented as mean ± standard deviation. For statistical analysis, the SAS (Cary, NC) software package JMP version 6.0 was used for data interpretation and graphic image design. RSM was used for modeling and analysis for the variables of the electrospinning process investigated in this work. Surface response diagrams allow the outline of specific parameters of the operating system and display the optimum set of parameters for the response. Thus the process yield is a function of the levels of interest where $y = f(x_1 + x_2) + \varepsilon$, where y is the process yield, x_1 and x_2 are the factors at the level of interest, ε is the error observed in the response. By denoting $E(y) = f(x_1 + x_2) = \eta$, then this surface represented by $\eta = f(x_1 + x_2)$.[28] Generally the second-order model is used for RSM where $y = \beta_0 + \sum\beta_i x_i + \sum\beta_{ii}^2 x_i + \sum\sum\beta_{ij} x_i x_j + \varepsilon$ when $i = 1$ to k and $i < j$, where β are the coefficients, x_i are the variables of interest, k is the level of factors, and ε is the observed error in the response, y.[28] The parameters and values for each parameter are shown in Table I.

RESULTS AND DISCUSSION

Effect of polymer concentration

Electrospinning proves to be a very complex process dependent on numerous variables. The initial investigation was pertinent to determine the appropriate polymer concentration to obtain highly uniform electrospun fibers before the addition of MWNT. PLA weight percentages of 5, 10, and 20 were investigated with favorable results for the higher concentrations of PLA in chloroform. Figure 1 shows the PLA morphology as a function of concentration electrospun at 15 kV and 10 cm at a flow rate of 100 μL/min. At 5 wt % PLA porous beads were produced, because the concentration of the polymer was too low to allow chain entanglements to occur. At 10 wt % PLA, inconsistent fibers were produced, which was followed up by the electrospinning of 20 wt % PLA. This concentration produced homogeneous nanofibers with a distribution of fiber diameters. Shenoy et al. was able to determine the role of chain entanglements on fiber formation for electrospinning by characterizing the number of entanglements per chain (n_e).[17] For a polymer solution,

$$(n_e)_{\text{soln}} = (\varphi_p \times M_w)/(M_e)_{\text{soln}} \tag{2}$$

TABLE I
Design of Experiment for Electrospinning of PLA with MWNT

Operating parameter	Range
Flow rate	50–200 μL/min
Applied voltage	10–20 kV
Working distance	10–20 cm
Solvent system	C or C/DMF
MWNT wt %	0–1 wt %

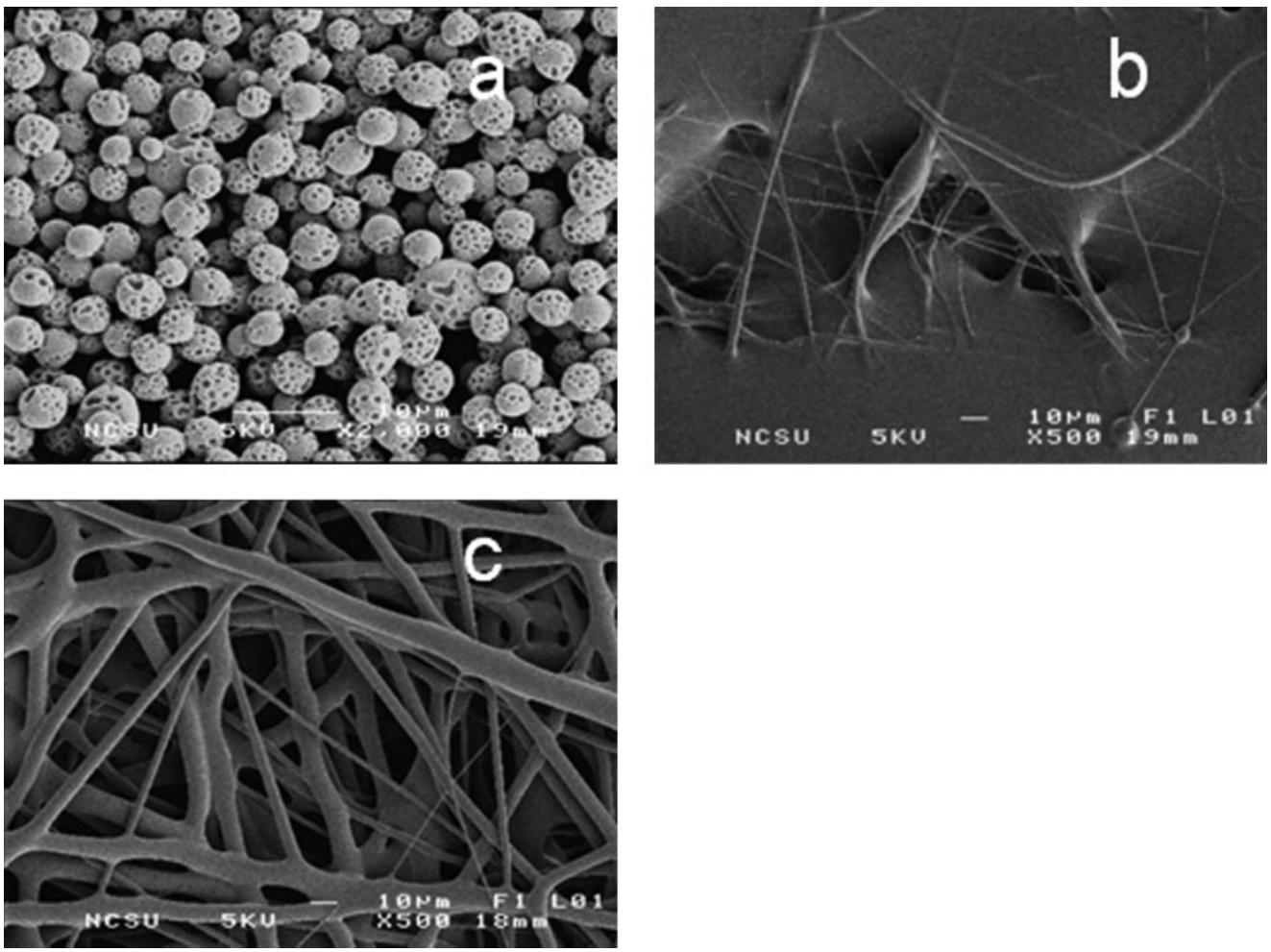

Figure 1 SEM images of electrospun PLA at (a) 5 wt % (b) 10 wt % and (c) 20 wt % PLA.

Here M_w is the molecular weight of the polymer, M_e is the entanglement molecular weight, and φ_p is the volume fraction or concentration of polymer. The number of chain entanglements per chain (n_e) must be equal to or greater than 3.5 for complete stable fiber formation.[17] The M_e of PLA has been reported to be 8000 g/mol, and represents the average molecular weight between chain entanglements.[29] Shenoy et al. was able to compile estimations and experimental observations for entanglement concentration of the polymer in solution for PDLA and PLLA (M_w of 109,000 and 670,000 g/mol, respectively). For the PDLA, the estimated concentration for fiber formation without beading is 32 wt %. This estimation was valid by fiber formation for PDLA being in the range of 30–35 wt %. The PLLA entanglement concentration estimation (n_e) ranged from 3.4 to 4 and was validated experimentally. In this study, the PLA has a M_w of 250,000 g/mol and as seen in Figure 1, we were able to produce fibers at 20 wt %. For our system, the minimum PLA concentration needed to spin continuous fibers is 11.2 wt % ($n_e = 3.5$). When calculating n_e as seen in Table II, n_e is 1.56 for a weight fraction of 5% which agrees with Shenoy's

TABLE II
Estimated Chain Entanglements Per Chain Based on Molecular Weight, Entanglement Molecular Weight, and Volume Fraction

Molecular weight (g/mol)	Entanglement molecular weight (g/mol)	Weight (%)	Volume fraction (φ_p)	Estimated chain entanglements/ Chain (n_e)
250,000	8000	5	5%	1.56
250,000	8000	10	9%	2.81
250,000	8000	20	17%	5.2

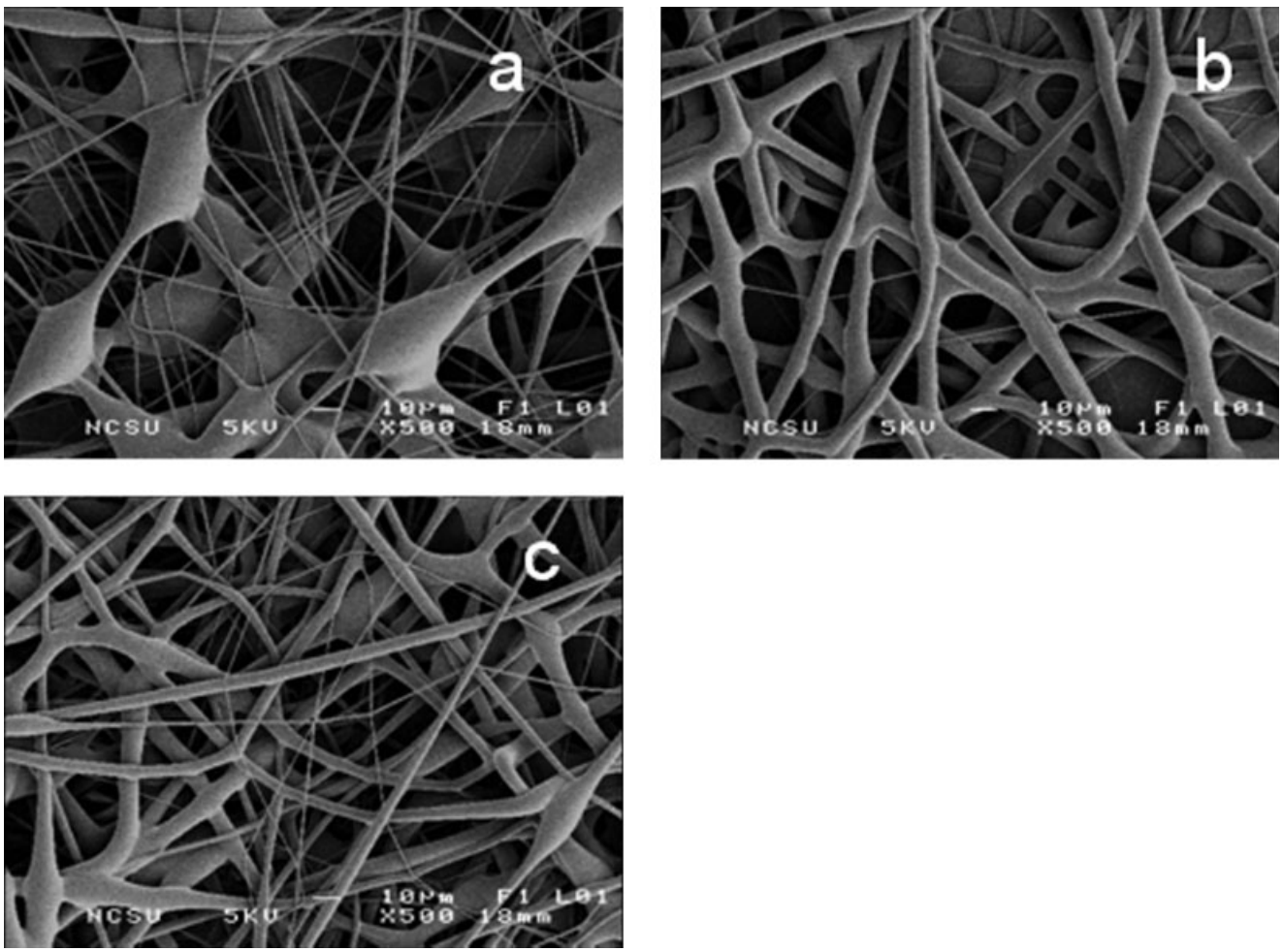

Figure 2 SEM images of electrospun PLA at applied voltages of (a) 10, (b) 15, and (c) 20 kV.

model for bead formation and with our morphology as shown in Figure 1(a). When the weight fraction was raised to 10%, we obtained an n_e of 2.82 and were unable to produce uniform fully developed fibers as seen in Figure 1(b) as the theory predicts. To overcome this, we increased the weight fraction of polymer to 20% where n_e is 5.0, and were able to produce uniform fibers with no beading. Though this entanglement concentration seems high and produced micron sized fibers, we believe that we can minimize the fiber diameter and maximize the surface area for the electrospun scaffolds by optimizing the processing parameters including flow rate (mL/min), applied voltage (kV), and working distance (cm).

Effect of flow rate

After determining the concentration of polymer at 20 wt %, the flow rate of the polymer solution was evaluated (at 20 wt %) holding voltage and working distance constant at 15 kV and 10 cm, respectively. It was observed that at flow rates below 100 μL/min the chloroform would evaporate quickly, and tend to clog the syringe needle at all electric field settings. Flow rates above 100 μL/min led to an unstable jet because the Taylor cone did not form properly because of the volume of polymer solution being too large and the viscosity being too low, at all electric field settings. Thus it was determined that the optimum flow rate for PLA was 100 μL/min to generate a continuous stream with minimal clogging.

Effect of voltage

Using a concentration of 20 wt %, a working distance of 10 cm, and flow rate of 100 μL/min the effect of voltage was evaluated at 10, 15, and 20 kV. We were unable to generate continuous fibers below 10 kV. Figure 2 shows the morphological changes as a function of the applied voltage. At 10 kV, fibers with a mean diameter of 1.98 ± 1.10 μm were produced but with beads and films apparent. At 15 kV, fibers with a mean diameter of 2.11 ± 2.17 μm were consistently formed, with a reduction in films and beads. At 20 kV, it was determined that a higher average density of fibers over the sample area was pro-

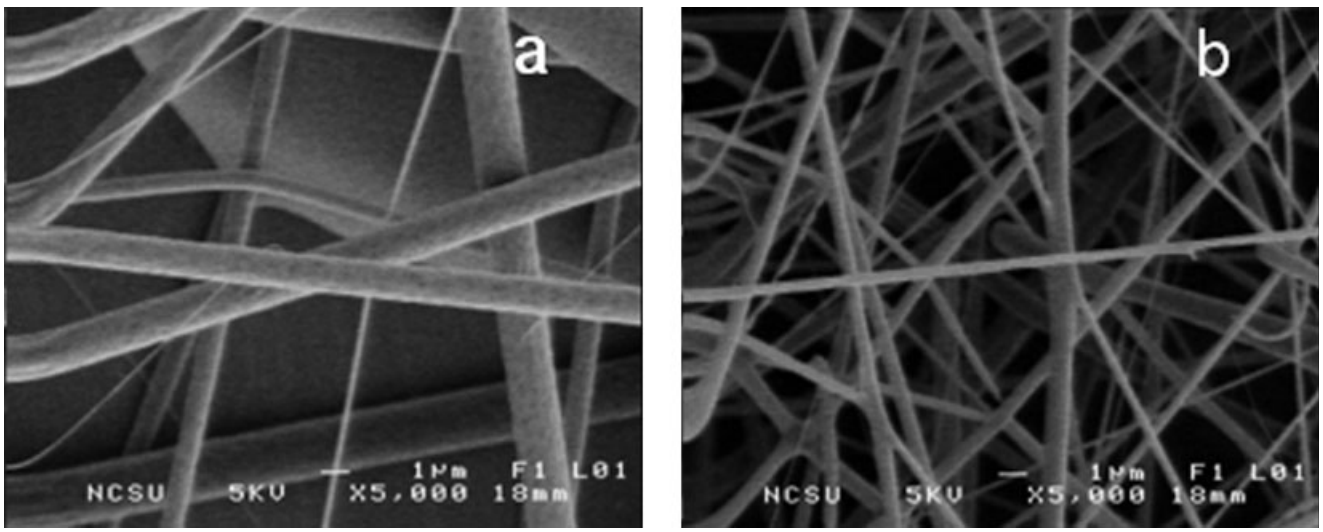

Figure 3 SEM images of electrospun PLA in (a) chloroform and (b) chloroform/DMF (3 : 1).

duced through SEM analysis. Past work by Zong et al. examined the effects of voltages above 20 kV and determined that with increasing intervals of 5 kV, beaded fibers are produced as a result of the Taylor cone being unstable which can result in non-uniform fibers.[23] Thus 15 and 20 kV served as the optimum voltage range for further testing when analyzing the effect of the working distance.

Effect of working distance

After determining an optimum spinning voltage, the distance from the syringe tip to the collector plate was investigated at measurements of 10, 15, and 20 cm maintaining a polymer concentration of 20 wt %, flow rate of 100 μL/min and voltage of 15 and 20 kV. Distances below 10 cm yielded no nanofibers and only thick films, while distances greater than 20 cm proved to be inefficient in collecting the charged jets of fibers. As the working distance increased from 10 to 15 cm smaller fibers were produced by extending the whipping distance of the polymer jet. Hence, it was determined that 15 cm provided the optimal spacing for the electrospinning of PLA to achieve the smallest fiber diameter and to maximize the surface area of the scaffold.

Effect of solvent system

Until this point, chloroform was the solvent used. In preparation for the addition of MWNT, the effects of two different solvent systems were investigated. Using the aforementioned processing parameters (15 kV, 15 cm, 100 μL/min), the pure PLA and chloroform solution created fibers with a mean diameter of 2.51 ± 2.13 μm for all processing conditions. With the addition of DMF, the fiber diameter was reduced dramatically as can be viewed in Figure 3. This is

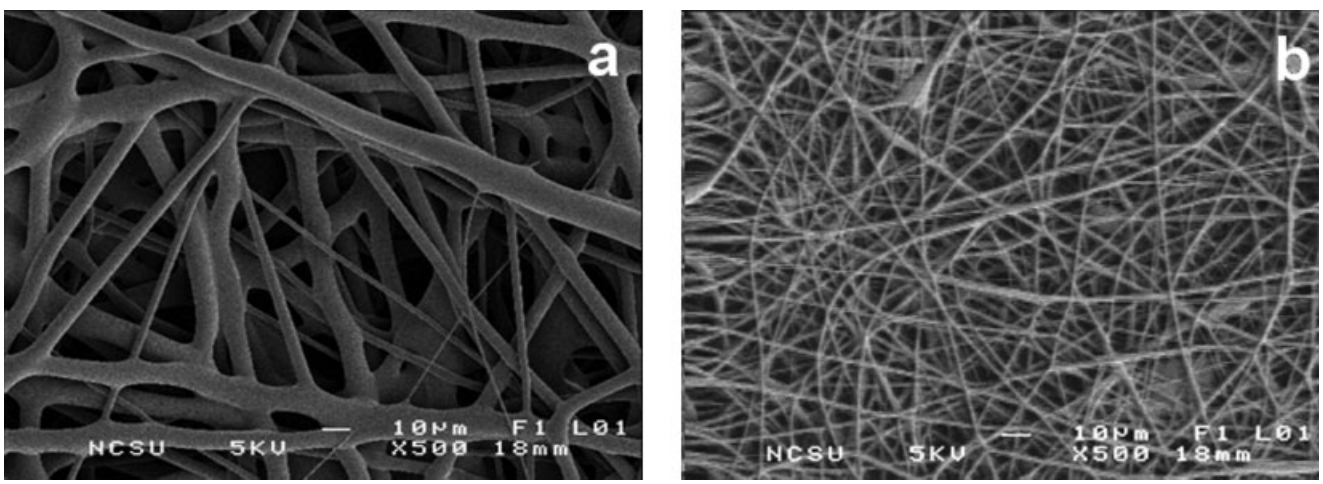

Figure 4 SEM images of electrospun (a) PLA and (b) 1 wt % MWNT/PLA.

TABLE III
Electrospinning Parameters and Fiber Diameters for PLA and MWNT/PLA Nanofibers

MWNT (wt %)	Working distance (cm)	Applied voltage (kV)	Mean fiber diameter (μm)	Standard deviation (μm)
0	10	10	1.98	0.2
0	10	15	2.77	0.19
0	10	20	2.96	0.21
0	15	15	0.55	0.05
0	15	20	0.79	0.09
1	10	15	0.79	0.08
1	10	20	0.96	0.06
1	15	15	0.56	0.05
1	15	20	0.55	0.05
1	20	15	0.65	0.09
1	20	20	0.86	0.12

All solutions were in the solvent system of Chloroform and DMF at a ratio of 3 : 1 respectively and at a flow rate at 100 μL/min.

attributed to the addition of another solvent, where the volatile properties of chloroform at room temperature are abated. By adding DMF to chloroform, the syringe needle experienced less clogging and was able to maintain a more stable jet without intervention. With the Chloroform/DMF solvent system at a ratio of 3 : 1, fibers with smaller diameters were produced by DMF enabling stable jets from the needle to the collector. We confirm that DMF is needed in the spinning solution that agrees with previous studies.[23]

Effect of MWNT addition

By incorporating the MWNT into the polymer solution, the solution behaved somewhat differently when compared to the PLA polymer solution for the same processing parameters. The MWNT/PLA solution appeared to produce fibers much more rapidly as seen by visual inspection. This can be attributed to the conductivity of the MWNT, which can increase the conductivity of the solution, or maintain a more uniform charge density on the fiber surface as hypothesized by Zang et al.[21] It can be postulated that there is a significant interaction between the MWNT and the PLA during electrospinning as the Taylor cone forms. The addition of MWNT is not only able to increase the conductance of the spinning solution, but also allow the fibers to crystallize around them when collected, as hypothesized by Zang et al.[21] In Figure 4, the SEM images of electrospun PLA show the dramatic decrease in fiber diameter with the addition of 1 wt % MWNT. For each SEM image, fiber diameters were calculated using the Scion Image™ software. In Table III, the processing variables and resulting fiber diameters are compiled.

When analyzing the SEM images of the MWNT/PLA fibers, the fibers appear to form a more densely interconnected network and produce significantly smaller fibers by a reduction of ~ 70% compared to pure PLA fibers. Histogram charts were developed using the data obtained from Scion Image™ software, and inputted directly into the JMP 6.0 software for statistical analysis. Figures 5 and 6 confirm the fiber diameter distributions where 67.9% of the PLA fibers are greater than 1 μm in diameter (Fig. 5), where 82.9% of the MWNT/PLA fibers are less than 1 μm in diameter (Fig. 6) where the percentage is simply the frequency of the fiber diameters. Both data sets have skewed data and do not fit a normal distribution. With the addition of the MWNT we are able to increase the charge density and produce a more uniform fiber distribution. To qualify that there is a statistical difference between the two data sets, a Wilcoxon/Kruskal-Wallis Test was performed

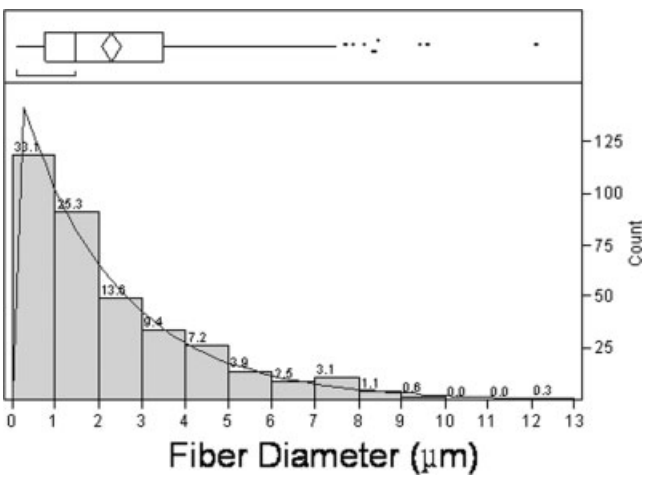

Figure 5 Distribution of fiber diameters for electrospun PLA.

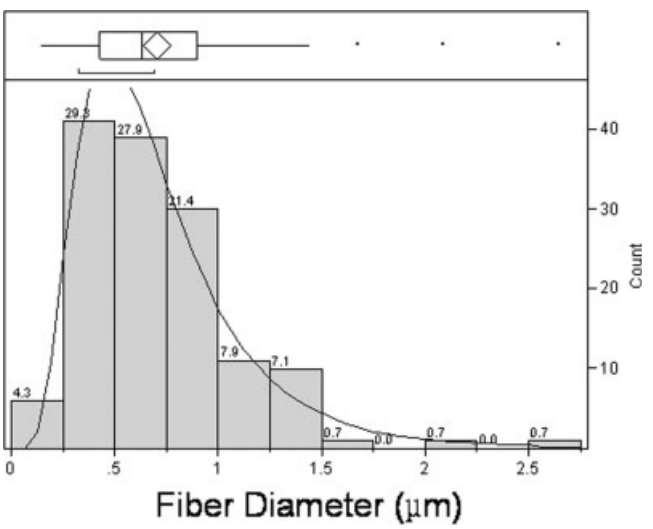

Figure 6 Distribution of fiber diameters for electrospun MWNT/PLA.

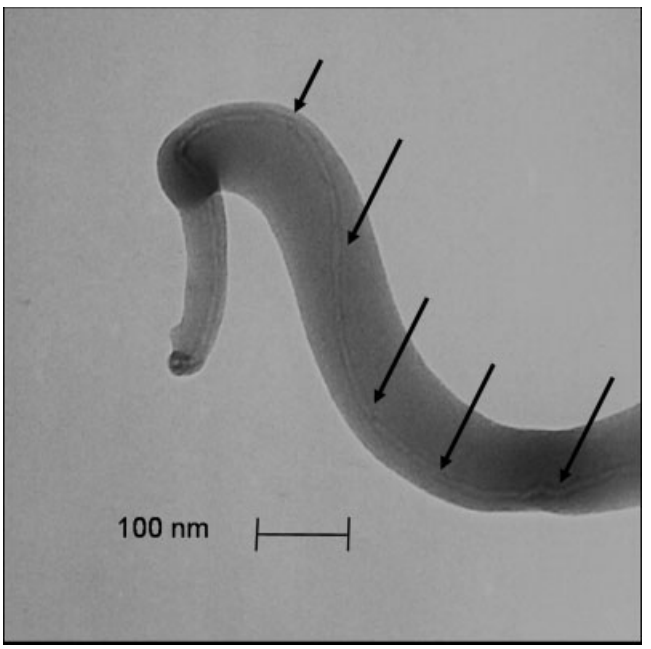

Figure 7 TEM images of electrospun MWNT/PLA.

because the data are nonparametric. Because the data is nonparametric and distributed differently, the test analyzes the median values of each set, not the mean. This measure of analysis returned a *P*-value less than 0.05 which designates the data is statistically different and that the addition of MWNT is able to produce fibers consistently smaller than pure PLA fibers.

High-resolution TEM images were taken to determine the orientation of the MWNT within the electrospun fibers. The fibers for PLA and MWNT/PLA were deposited on individual TEM grids during the electrospinning process. The MWNT were oriented along the axis of the fibers, and are shown in Figure 8. When viewing Figure 7, we can see that the MWNT is completely dispersed and aligned within the fiber and that no agglomeration is taking place.

RSM is a useful technique for examine the response of interest for a specific system. By analyzing the effects of the electric field, *E* (kV/cm) and presence of MWNT, a surface response diagram and contour plot can be produced. This type of analysis provides a means to take into account the combined effects of multiple variables and determine a response. Surface response diagrams allow the user to outline specific parameters of the operating system and display the optimum set of parameters for the response. The surface response diagram or contour plot of the predicted fiber diameter can be developed based on the data set obtained and will provide contour curves to illustrate where significant changes take place in the production of electrospun PLA fibers. In Figure 8, for pure PLA, applied voltage and working distance are plotted to illustrate their apparent effect on fiber diameter. Fiber diameter is strongly affected by both the applied voltage and working distance, decreasing when both of the variables are increased. In MWNT/PLA nanofibers it can be seen that with a minimum working distance of 13 cm and an applied voltage equal to or greater than 15 kV, fibers can be produced with diameters equal to or less than 700 nm (as shown in Fig. 9). Therefore, this contour plot indicates a wide processing range for the production of submicron fibers.

Fourier transform infrared spectroscopy

FTIR was employed to determine if there were any residual solvents within the electrospun samples. The samples were not further processed after electrospinning.

Figure 10(a) shows an FTIR spectrum for a control sample of as-received PLA (represented by the blue

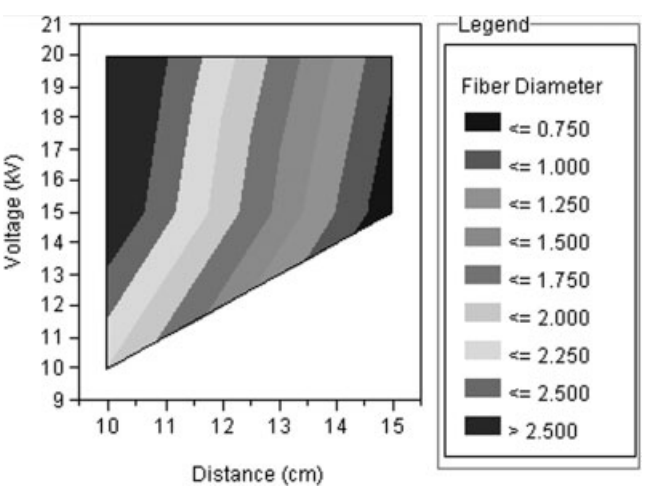

Figure 8 Contour plot for electrospun PLA fiber diameters (in μms).

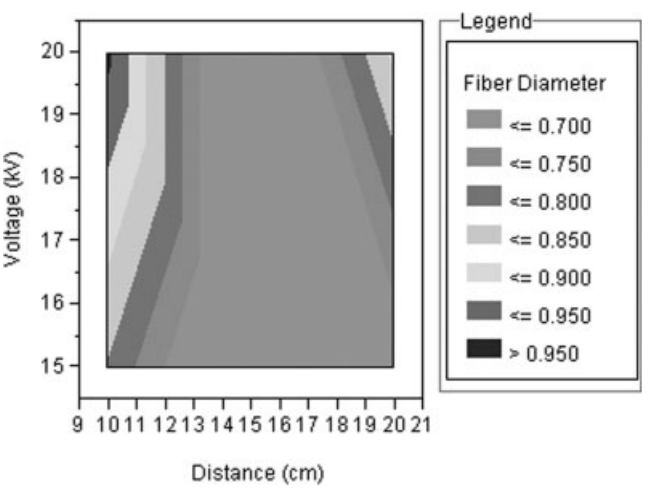

Figure 9 Contour plot for electrospun MWNT/PLA fiber diameters (in μms).

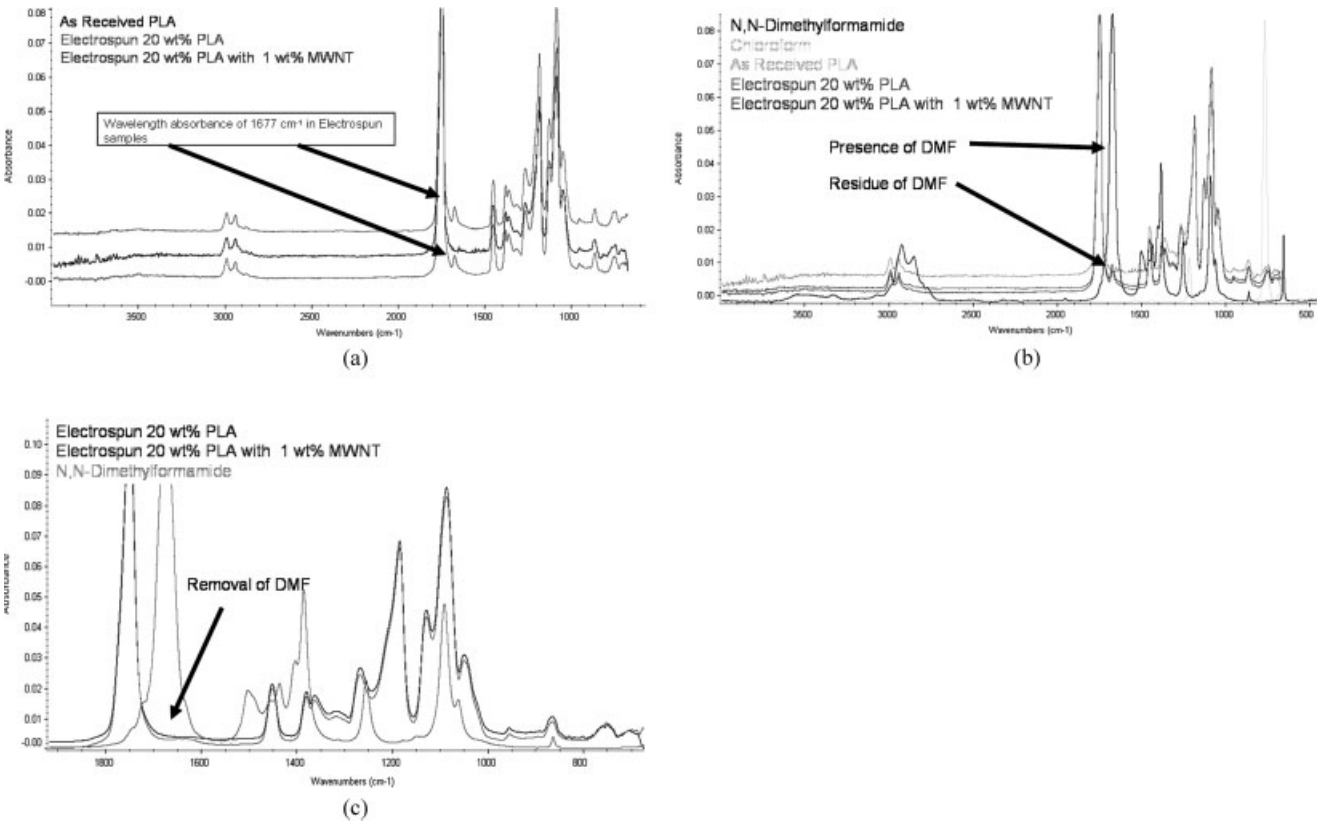

Figure 10 FTIR absorbance spectrum for (a) PLA, (b) PLA (before washing) and solvents, and (c) PLA (after washing with PBS) and solvents.

absorbance plot). The electrospun PLA with and without MWNT are indicated by the green and red absorbance plots, respectively. The electrospun samples have the same absorbance as the control PLA with the addition of a small perturbation at 1677 cm^{-1} indicated by the arrows. When comparing the electrospun samples to the absorbance spectrums of the solvents chloroform and *N*-*N*-DMF, it is apparent that there is no residue of chloroform retained in the sample as seen in Figure 10(a). However, there appears to be a residue of *N*-N-DMF which is indicated by the 1677 cm^{-1} and can be seen in Figure 10(b). For this absorbance, it could be either indicative of a carbonyl group or a primary amine. The molecular structure of DMF is an amide compound. Thus, the absorbance at the wavelength is due to a slight presence of the DMF left in the electrospun samples. After washing the electrospun scaffold in PBS we were able to remove the DMF as seen in Figure 10(c).

Electrical measurements on random mats

In previous studies of artificial tissue growth, electrical stimulation from capacitive plates in solution,[30] direct current flow through a conducting scaffold,[31] or a combination of both[32] have shown effective in increasing cell proliferation. Reorientation of cells in response to an applied electric field has also been observed.[33] Thus the addition of MWNT to electrospun PLA not only dramatically reduces fiber size, which more closely resembles the extracellular matrices found *in vitro*, but also provides a mechanism to tune the electrical characteristics of the resulting tissue scaffold. Tissue scaffolds would be formed of random mats of MWNT-doped electrospun fibers. Thus we measure the electrical conductance of such random mats as a function of doping, as shown in Figure 11. The data is shown versus the experimentally controlled parameter (MWNT/PLA wt % in solution) as well as nanotube volume percentage in the full composite (voids, polymer, and MWNT), which is obtained via analysis of SEM images of mats at each weight percentage. (see also, Ref. 27) Because the fiber size ($\sim$ 700 nm) and porosity of the composite (87%) do not change as a function of increasing MWNT doping, the two axes are related by a simple scaling factor for small MWNT wt %.

The incorporation of a conducting filler (MWNT) into an insulating matrix (PLA) leads to a strongly nonlinear increase in conductivity as a function of doping. This effect is often described by classical percolation theory.[34] In short, the composite material does not become conducting until a critical density

of dopant occurs where neighboring filler particles overlap, providing a path for current across the sample. After a dramatic increase near this ''percolation threshold,'' where many interconnecting paths branch out to fill the entire sample volume, further doping leads to little increase in conductance and saturation at a maximum conductivity is observed.

Figure 11 shows such percolation behavior, which can be quantified by fitting with various models. We are particularly interested in two characteristics of the electrical behavior. First, to minimize cost and any adverse biomedical effects of the MWNT, utilizing a minimal level of MWNT doping will be prudent in any application. Thus we are interested in determining the critical density of MWNT needed for conductivity and how this parameter varies with mat morphology.[27] Second, the minimum scaffold conductivity needed for electrical stimulation has been estimated as $\sim 10^{-3}$ S/cm.[35] Thus, we wish to compare our maximum conductivity with this limit.

Two models are utilized to fit the data. The fit after Fournier, which encompasses all data points, yields a percolation threshold of 0.30 ± 0.03%.[36] A traditional fit from percolation theory $G \sim (p - p_c)^t$ where p is the MWNT wt %, p_c the critical doping level and t, a fitting exponent, applies only to data above threshold and yields [$p_c = (0.30 \pm 0.05)\%$].

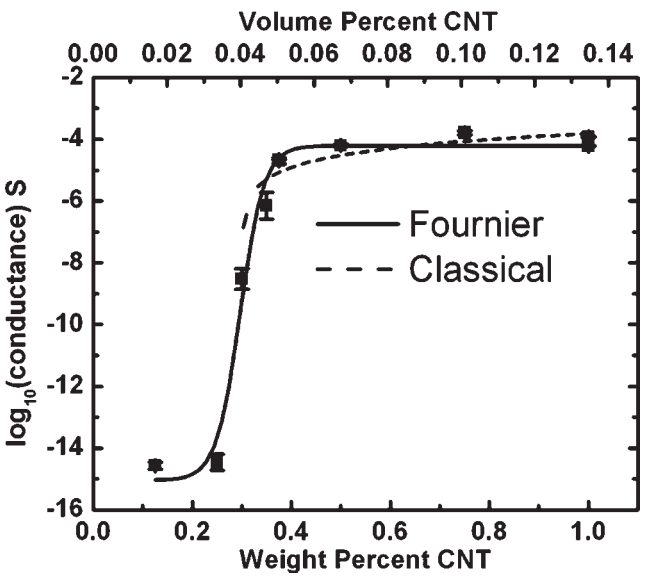

Figure 11 Electrical conductance of random mats of PLA : MWNT fibers as a function of MWNT doping. The conductance is plotted versus the weight percent of nanotubes in the spinning solution (the experimental variable) as well as the observed volume fraction of nanotubes in the resulting mat. For the latter, SEM images of each conductance sample determined the porosity of the mat and the resulting MWNT volume fraction was calculated. At wt % values of 0.375 and 1, two samples are represented. The two fits and the resulting parameters are described in the text.

TABLE IV
Mechanical Properties of MWNT/PLA Nonwoven Mats

Sample (MWNT) wt %	Modulus (MPa)	Yield strength (MPa)
0	14.87 ± 2.93	2.07 ± 0.097
0.25	55.35 ± 5.95	1.54 ± 0.04
0.50	25.24 ± 5.35	1.38 ± 0.057
1	11.17 ± 3.98	1.99 ± 0.054

Taking into account the interdigitated geometry of the sample (effective sample size 51 mm × 1 μm × 10 μm) and the observed porosity, an order of magnitude estimate of the conductivity yields $\sigma \sim 1 \times 10^{-3}$ S/cm, which should be adequate for electrical stimulation. The observed critical doping levels of ~ 0.30 MWNT wt % fall between that reported for a single, larger diameter fiber ($p_c < 0.05\%$) and typical values for films (~ 10–20%) but generally provide for adequate conductivity with limited doping. Finally, the fitting exponent $t = 1.3 \pm 0.8$ is a measure of the dimensionality of the system and, as we previously reported, may indicate the effect of the constraints of the fiber geometry.[27]

Tensile measurements on random mats

Tensile tests were performed to determine any changes in mechanical properties because of MWNT concentrations of 0, 1, 0.25, 0.50, and 1 wt %. For each sample measured, the thickness was determined by the mean of 10 measurements per sample. Each sample was collected from the plate collector and removed from the aluminum foil. The results are shown in Table IV. The stress calculation accounts for the void volume fraction in pure PLA (75%) and all samples containing MWNT (87%). The 0.25 wt % MWNT/PLA sample maintained the same tensile stress yet had a statistically significant increase in modulus when compared to the pure PLA sample. However, the 1 wt % MWNT/PLA sample demonstrated a reduction in modulus. This can be attributed to agglomeration of MWNT at the higher concentration, which could limit the effective surface area available for load transfer.

CONCLUSIONS

From this investigation it has been determined that the optimal concentration of PLA with M_w 250,000 g/mol is ~ 20 wt % producing a chain entanglement value (n_e) of 5.20 for proper fiber formation. This concentration produces fibers with no beading or film formation. Also, the optimum processing parameters for this concentration are an applied voltage of 15 kV and a working distance of 15 cm. The preferred solvent system is a combination of chloroform and DMF to reduce the volatile action of chlo-

roform. FTIR has indicated that there is a residual of DMF on the electrospun samples but chloroform is not present. With the addition of 1 wt % MWNT, the fiber diameter is drastically reduced by 70% to form fibers with a mean diameter of 700 nm in the processing range between 13 and 18 cm working distance and a voltage of 15–20 kV. TEM has validated the alignment of the MWNT within the fibers. Young's modulus was maximized at a loading level of 0.25 wt %. The percolation threshold for electrical conductivity also occurs near this value at 0.30 wt %.

The author thank Ms. Birgit Anderson, Mr. Alfred Inman, and Dr. Dale Batchelor for their technical assistance.

References

1. Harris, P. J. F. Int Mater Rev 2004, 49, 31.
2. Hussain, F.; Hojjati, M.; Okamot M.; Gorga, R. E. J Compos Mater 2006, 40, 1511.
3. Moniruzzaman, M.; Winey, K. I. Macromolecules 2006, 39, 5194.
4. Ponomarenko, A. T.; Shevchenkoand, V. G.; Enikolopyan, N. S. Adv Polym Sci 1990, 96, 125.
5. Gorga, R. E.; Cohen, R. E. J Polym Sci Part B: Polym Phys 2004, 42, 2690.
6. Dondero, W. E.; Gorga, R. E. J Polym Sci Part B: Polym Phys 2006, 44, 864.
7. Mack, J. J.; Viculis, L. M.; Ali, A.; Luoh, R.; Yang, G. L.; Hahn, H. T.; Ko, F. K.; Kaner, R. B. Adv Mater 2005, 17, 77.
8. Saeed, K.; Park, S. Y.; Lee, H. J.; Baek, J. B.; Huh, W. S. Polymer 2006, 47, 8019.
9. Salalha, W.; Dror, Y.; Khalfin, R. L.; Cohen, Y.; Yarin, A. L.; Zussman, E. Langmuir 2004, 20, 9852.
10. Sawicka, K. M.; Gouma, P. J Nanoparticle Res 2006, 8, 769.
11. Sen, R.; Zhao, B.; Perea, D.; Itkis, M. E.; Hu, H.; Love, J.; Bekyarova, E.; Haddon, R. C. Nano Lett 2004, 4, 459.
12. Formhals, A. US Pat. 1,975,504 (1934).
13. Li, D.; Xia, Y. Adv Mater 2004, 16, 1151.
14. Li, C.; Vepari, C.; Jin, H.-J.; Kim, H. J.; Kaplan, D. Biomaterials 2006, 27, 3115.
15. Inai, R.; Kotaki, M.; Ramakrishna, S. Nanotechnology 2005, 16, 208.
16. Pham, Q. P.; Sharma, U.; Mikos, A. G. Tissue Eng 2006, 12, 1197.
17. Shenoy, S. L.; Bates, W. D.; Frisch, H. L.; Wnek, G. E. Polymer 2005, 46, 3372.
18. Tan, S.-H.; Inai, R.; Kotak, I. M.; Ramakrishna, S. Polymer 2005, 46, 6128.
19. Xiaoyi, X.; Qingbiao, Y.; Yongzhi, W.; Haijun, Y.; Xuesi, C.; Xiabin, J. Eur Polym J 2006, 42, 2081.
20. Yoshimoto, H.; Shin, Y. M.; Terai, H.; Vacanti, J. P. Biomaterials 2003, 24, 2077.
21. Zeng, J.; Xu, X.; Chen, X.; Liang, Q.; Jing, X.; Yang, L.; Bian, X. J Controlled Release 2003, 92, 227.
22. Zong, X. H.; Bien, H.; Chung, C. Y.; Yin, L. H.; Fang, D. F.; Hsiao, B. S.; Chu, B.; Entcheva, E. Biomaterials 2005, 26, 5330.
23. Zong, X. H.; Kim, K.; Fang, D. F.; Ran, S. F.; Hsiao, B. S.; Chu, B. Polymer 2002, 43, 4403.
24. Ren, Z. F.; Huang, Z. P.; Xu, J. W.; Wang, J. K.; Bush, P.; Siegel M. P.; Provencio, P. Science 1998, 282, 1105.
25. Monteiro-Riviere, N.; Inman, A.; Wang, Y.; Nemanich, R. Nanomed Nanotechnol Biol Med 2005, 1, 293.
26. Moore, V. C.; Strano, M. S.; Haroz, E. H.; Hauge, R. H.; Smalley, R. E. Nano Lett 2003, 3, 1379.
27. McCullen, S. D.; Stevens, D. R.; Roberts, W. A.; Ojha, S. S.; Clarke, L. I.; Gorga, R. E. Macromolecules, accepted.
28. Montgomery, D. C. Design and Analysis of Experiments; Wiley: Hoboken, 2005.
29. Cooper-White, J.; Mackay, M. J Polym Sci Part B: Polym Phys 1999, 37, 1803.
30. Pedrotty, D. M.; Koh, J. Am J Physiol Heart Circ Physiol 2005, 288, 1620.
31. Kotwal, A.; Schmidt, C. E. Biomaterials 2001, 22, 1055.
32. Supronowicz, P. R.; Ajayan, P. M.; Ullmann, K. R.; Arulanandam, B. P.; Metzger, D. W.; Bizios, R. J Biomed Mater Res 2002, 59, 499.
33. Sun, S.; Titushkin, I.; Cho, M. Bioelectrochemistry 2006, 69, 133.
34. Stauffer, D.; Aharony, A. Introduction to Percolation Theory; Taylor and Francis: Washington, DC, 1992.
35. Wan, Y.; Wu, H.; Wen, D. Macromol Biosci 2004, 4, 882.
36. Fournier, J.; Boiteux, G.; Seytre, G.; Marichy, G. Synth Metals 1997, 84, 839.